Journal of Controlled Release 193 (2014) 154–161

Contents lists available at ScienceDirect

Journal of Controlled Release

journal homepage: www.elsevier.com/locate/jconrel

Galactose-installed photo-crosslinked pH-sensitive degradable micelles for active targeting chemotherapy of hepatocellular carcinoma in mice

Yan Zou [a], Yuan Song [b], Weijing Yang [a], Fenghua Meng [a,*], Haiyan Liu [b], Zhiyuan Zhong [a,*]

[a] Biomedical Polymers Laboratory, and Jiangsu Key Laboratory of Advanced Functional Polymer Design and Application, College of Chemistry, Chemical Engineering and Materials Science, Soochow University, Suzhou 215123, China
[b] Laboratory of Cellular and Molecular Tumor Immunology, Cyrus Tang Hematology Center, Medical College, Soochow University, Suzhou 215123, China

ARTICLE INFO

Article history:
Received 14 March 2014
Accepted 7 May 2014
Available online 20 May 2014

Keywords:
Degradable micelles
pH-sensitive
Crosslinked micelles
Hepatocellular carcinoma
Galactose

ABSTRACT

In this study, we designed and developed galactose-installed photo-crosslinked pH-sensitive degradable micelles (Gal-CLMs) for active targeting chemotherapy of hepatocellular carcinoma in mice. Gal-CLMs were readily obtained from co-self-assembly of poly(ethylene glycol)-*b*-poly(mono-2,4,6-trimethoxy benzylidene-pentaerythritol carbonate-*co*-acryloyl carbonate) (PEG-*b*-P(TMBPEC-*co*-AC)) and Gal-PEG-*b*-poly(ε-caprolactone) (Gal-PEG-*b*-PCL) copolymers followed by photo-crosslinking. Notably, paclitaxel (PTX)-loaded Gal-CLMs (Gal-PTX-CLMs) showed a narrow distribution (PDI = 0.08–0.12) with average sizes ranging from 92.1 to 136.3 nm depending on the Gal contents. The release of PTX from Gal-CLMs while inhibited at physiological pH was enhanced under endosomal pH conditions. MTT assays in asialoglycoprotein receptor (ASGP-R) over-expressing HepG2 cells demonstrated that half-maximal inhibitory concentration (IC_{50}) values of Gal-PTX-CLMs decreased from 11.7 to 2.9 to 1.1 μg/mL with increasing Gal contents from 10% to 20% to 30%, supporting receptor-mediated endocytosis mechanism. The *in vivo* biodistribution studies in human hepatoma SMMC-7721 tumor-bearing nude mice displayed that Gal20-PTX-CLMs resulted in significantly enhanced drug accumulation in the tumors over non-targeting PTX-CLM counterpart. In accordance, Gal20-PTX-CLMs caused much greater tumor growth inhibition than non-targeting PTX-CLMs as well as non-crosslinking Gal20-PTX-NCLM controls (average tumor volume: *ca.* 35 mm^3 *versus* 144 mm^3 and 130 mm^3, respectively). Histological analysis showed that Gal20-PTX-CLMs induced more extensive apoptosis of tumor cells while less damage to normal liver and kidney compared to Taxol. Ligand-installed photo-crosslinked pH-responsive degradable micelles have a great potential for targeted cancer chemotherapy.

1. Introduction

Biodegradable micelles based on aliphatic polyesters and polycarbonates are one of the most promising nanosystems for the controlled and targeted delivery of potent lipophilic anticancer drugs such as paclitaxel (PTX) and doxorubicin (DOX) [1–4]. However, the therapeutic efficacy of current degradable micellar drug formulations remains low due to barriers of low *in vivo* stability, poor tumor cell uptake, and/or slow drug release inside tumor cells [5,6]. It should in particular be noted that there exist two pairs of conflicting requirements for efficient cancer chemotherapy, *i.e. in vivo* stability *versus* intracellular drug release and stealth property *versus* tumor cell uptake.

A high *in vivo* stability is important in order to avoid premature drug release, enhance tumor targetability and decrease systemic side effects [7–9]. On the other hand, to illicit a therapeutic effect, drug has to be released once being transported into target tumor cells [10,11]. The fast intracellular drug release might also help to effectively overcome multidrug resistance (MDR) [12–14]. In the past years, reversibly crosslinked degradable micelles [15–22] and crosslinked pH-sensitive degradable micelles [23,24] have been designed to resolve the *in vivo* stability and intracellular drug release dilemma. These reversibly crosslinked micelles while displaying inhibited drug release under a physiological environment are able to quickly release drugs inside tumor cells as a result of micelle de-crosslinking and dissociation under an intracellular reductive [15–20] or acidic condition [21,22], leading to enhanced *in vivo* cancer treatment efficacy over their non-crosslinked counterparts [18,19]. Notably, stably crosslinked acid-sensitive degradable micelles could also quickly release drugs inside tumor cells. Hennink et al. reported that core-crosslinked acid-labile DOX prodrug micelles based on mPEG-*b*-p(HPMAm-Lac_n) demonstrated better anti-tumor activity than free DOX in mice

* Corresponding authors. Tel./fax: +86 512 65880098.
E-mail addresses: fhmeng@suda.edu.cn (F. Meng), zyzhong@suda.edu.cn (Z. Zhong).

http://dx.doi.org/10.1016/j.jconrel.2014.05.016
0168-3659/

bearing B16F10 melanoma carcinoma [23]. We recently reported that core-crosslinked pH-sensitive degradable micelles based on PEG-*b*-poly(mono-2,4,6-trimethoxy benzylidene-pentaerythritol carbonate-*co*-acryloyl carbonate) (PEG-*b*-P(TMBPEC-*co*-AC)) while exhibiting high stability under physiological pH gave enhanced PTX release under endo/lysosomal pH conditions due to acidic hydrolysis of acetals [24].

In order to achieve a long circulation time, micelles are typically stealthed by non-fouling polymers like PEG, dextran, and poly(acrylic acid). The stealthy surface would, nevertheless, also impede uptake of micellar drugs by tumor cells, truncating therapeutic effects. The installation of a tumor specific targeting ligand such as folic acid [12,25], an antibody [26,27], cRGD [28,29], galactose/lactose [30,31], aptamer [32,33] and transferrin [34], on the surface of micelles could largely improve tumor cell uptake of micellar drugs. In particular, β-D-galactose (Gal), N-acetylgalactosamine and lactose that are specific targeting ligands to asialoglycoprotein receptor (ASGP-R) on mammalian hepatocytes provide a useful means for targeted chemotherapy of liver cancers [35–40]. Notably, galactosamine-PHPMA-GFLG-DOX (PK2) represents the first active tumor-targeting polymeric nanomedicine translated to the human clinical trials [41]. The clinical results showed that liver-specific DOX delivery is achievable using PK2 and targeting is witnessed in primary hepatocellular tumors. Inspired by these clinical results, we recently designed and explored galactose-decorated degradable micelles and polymersomes for hepatoma-targeting anticancer drug delivery *in vitro*[42,43] and *in vivo*[10].

In this paper, we report on Gal-installed photo-crosslinked pH-sensitive degradable micelles (Gal-CLMs) as an integrative nanovehicle for active targeting chemotherapy of hepatocellular carcinoma in mice (Scheme 1). Gal-CLMs were prepared from co-self-assembly of PEG-*b*-P(TMBPEC-*co*-AC) and Gal-PEG-*b*-PCL copolymers followed by photo-crosslinking. These innovative degradable micelles were designed with following unique features: (i) they are stable with inhibited drug leakage in the circulation due to covalent crosslinking of micellar core; (ii) they can be efficiently taken up by hepatocellular carcinoma cells *via* receptor-mediated endocytosis mechanism; and (iii) drug release can be activated in the mildly acidic endo/lysosomal compartments owing to acid-triggered hydrolysis of acetals in the micellar core. Here, effects of Gal ligand densities on targetability and antitumor activity toward hepatocellular carcinoma cells, biodistribution, and *in vivo* therapeutic efficacy of PTX-loaded Gal-CLMs in SMMC-7721 bearing nude mice were investigated.

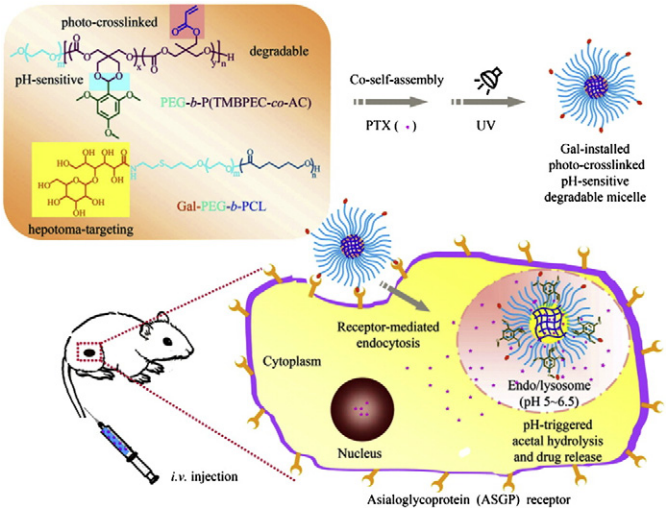

Scheme 1. Illustration of galactose-installed photo-crosslinked pH-sensitive degradable micelles based on PEG-*b*-P(TMBPEC-*co*-AC) and Gal-PEG-*b*-PCL copolymers as an integrative nanovehicle for active targeting chemotherapy of hepatocellular carcinoma in mice.

2. Materials and methods

2.1. Materials

Zinc bis[bis(trimethylsilyl)amide] (97%, Aldrich), lactobionic acid (LBA, 97%, Acros), 1-[4-2-hydroxy ethoxy-phenyl]-2-hydroxy-2-methyl-1-propanone (Irgacure 2959, 98%, Sigma), Cy7 (Beijing Fanbo Biochemicals), and paclitaxel (PTX) (>99% and from Beijing Zhongshuo Pharmaceutical Technology Development Co., Ltd., PRC) were purchased and used as received. Methoxy poly(ethylene glycol) (PEG, M_n = 5.0 kg/mol) was obtained from Fluka and dried by azeotropic distillation from anhydrous toluene. Poly(ethylene glycol)-*b*-poly(mono-2,4,6-trimethoxy benzylidene-pentaerythritol carbonate-*co*-acryloyl carbonate) (PEG-*b*-P(TMBPEC-*co*-AC)) (M_n = 5.0–(3.6–0.6) kg/mol, PDI = 1.06) and galactose-PEG-*b*-poly(ε-caprolactone) (Gal-PEG-*b*-PCL) (M_n = 6.0–4.0 kg/mol, PDI = 1.3) block copolymers were synthesized according to our previous reports [10,24,42]. Dichloromethane (DCM) was dried by refluxing over CaH_2 under a nitrogen atmosphere. The dialysis membranes (Spectra/Pore, MWCO 12,000–14,000) were purchased from Spectrum Laboratories.

2.2. Synthesis of Cy7 labeled PEG-b-PCL diblock copolymer

Cy7-PEG-*b*-PCL was synthesized by carbodiimide chemistry. The coupling reaction of NH_2-PEG-*b*-PCL (16 mg, 1.5 μmol) and Cy7 (2 mg, 2.8 μmol) was carried out under stirring for 24 h in DMF (2 mL) in the presence of NHS (0.16 mg, 1.5 μmol), DCC (0.288 mg, 1.5 μmol) and DMAP (0.156 mg, 0.8 μmol). The product was isolated by precipitation from cold diethyl ether and dried at r.t. in vacuo and then purified by extensive dialysis against water (MWCO 3500) followed by lyophilization. Yield: 72%. The Cy7 substitution was determined to be 92% by fluorometry based on a standard curve derived from a series of free Cy7 with known concentrations.

2.3. Characterization

^{1}H NMR spectra were recorded on a Unity Inova 400 spectrometer operating at 400 MHz using deuterated chloroform ($CDCl_3$) as a solvent. The chemical shift was calibrated against residual solvent signals. The molecular weight and polydispersity index (PDI) of polymers were determined by a Waters 1515 gel permeation chromatograph (GPC) instrument equipped with two linear PLgel columns (500 Å and Mixed-C) following a guard column and a differential refractive-index detector. The measurements were performed using DMF as the eluent at a flow rate of 1.0 mL/min at 30 °C and a series of narrow polystyrene standards for the calibration of the columns. The micelle size was determined using dynamic light scattering (DLS) at 25 °C using Zetasizer Nano-ZS (Malvern Instruments) equipped with a 633 nm He–Ne laser using back-scattering detection. The amount of PTX was determined by HPLC (Waters 1525) with UV detection at 227 nm using a mixture of acetonitrile and water (v/v = 1/1) as a mobile phase. Transmission electron microscopy (TEM) was performed using a Tecnai G220 TEM operated at an accelerating voltage of 200 kV. The samples were prepared by dropping 10 μL of micelle dispersion on the copper grid followed by staining with phosphotungstic acid (1 wt.%).

2.4. Preparation of Gal-installed crosslinked micelles (Gal-CLMs)

Gal-CLMs were prepared in a similar way as reported [24] with slight modification. Typically, under stirring, 800 μL of phosphate buffer (PB, 10 mM, pH 7.4) was added dropwise to a 200 μL solution of PEG-*b*-P(TMBPEC-*co*-AC) and Gal-PEG-*b*-PCL copolymers in DMF (5.0 mg/mL). The resulting micelles were dialyzed against the same PB for 12 h (Spectra/Pore, MWCO 7000). The sizes were determined by DLS and CMC by fluorometry using pyrene as a fluorescence probe as described in previous reports [44–46].

The obtained micelles were crosslinked by adding 50 μL of Irgacure 2959 solution in acetone (final concentration of 0.05 wt.%), evaporating acetone for 3 h and irradiating by UV light (Intelli-Ray 400, Uvitron) at an intensity of 100 mW/cm^2 for 10 min. The stability of crosslinked micelles against extensive dilution, 10% FBS, or THF was studied using DLS by monitoring changes of particle size and size distribution.

2.5. Loading and pH-responsive release of PTX

PTX-loaded micelles were prepared by dropwise adding 800 μL of PB (10 mM, pH 7.4) to a solution of PEG-*b*-P(TMBPEC-*co*-AC) and Gal-PEG-*b*-PCL block copolymers in DMF (5.0 mg/mL, 200 μL) containing 110 μg of PTX (10 wt.% PTX), and dialyzing against PB (10 mM, pH 7.4) for 12 h at room temperature (MWCO 7000) with 5 times change of dialysis media to remove free PTX. The micelles were crosslinked as described above by UV irradiation. The release of PTX during the photo-crosslinking process was negligible. To determine drug loading content (DLC) and drug loading efficiency (DLE), 100 μL of PTX-loaded non-crosslinked micelle dispersion was freeze-dried, the residue was dissolved in acetonitrile, and the amount of PTX was determined by HPLC. DLC and DLE were determined according to the following formula:

$$\text{DLC (wt.\%)} = (\text{weight of loaded drug/total weight of loaded drug and polymer}) \times 100\%$$

$$\text{DLE (\%)} = (\text{weight of loaded drug/weight of drug in feed}) \times 100\%.$$

The release profiles of PTX from Gal20-PTX-CLMs were studied at 37 °C in two different media, *i.e.* acetate buffer (100 mM, pH 5.0) and PB (100 Mm, pH 7.4). The above prepared micelle dispersions were divided into three aliquots. The pH of micelle dispersions was adjusted to pH 5.0 using acetate buffer or maintained at pH 7.4 using PB. 1.0 mL of the above micelle dispersions (final concentration of 32 μg/mL) were immediately transferred to dialysis tubes (MWCO 12,000–14,000), which were immersed into 20 mL of corresponding buffer (10 mM). The release media were stirred at 37 °C. At desired time intervals, 7.0 mL of release media were taken out for HPLC measurements and replenished with an equal volume of fresh media. The amount of PTX was determined by HPLC. The release experiments were conducted in triplicate and the results presented are the average data.

2.6. Evaluation of hepatoma targeting of Gal-PTX-CLMs by MTT assays

The antitumor activity of PTX-loaded hepatoma-targeting crosslinked micelles (Gal-PTX-CLMs) in asialoglycoprotein receptor (ASGP-R) over-expressing human hepatoblastoma cell line (HepG2) was studied by MTT assays. HepG2 cells pretreated with free LBA (2 mg/mL) and MCF-7 cells (low ASGP-R expression) were used as negative controls. In brief, HepG2 or MCF-7 cells were plated in a 96-well plate (1×10^4 cells/well) under 5% CO_2 atmosphere at 37 °C in 90 μL of DMEM containing 10% FBS, 1% L-glutamine, and antibiotics penicillin (100 IU/mL), and streptomycin (100 μg/mL) for 24 h. The medium was aspirated and replaced by 90 μL of fresh medium. 10 μL of PTX formulations, Gal10-PTX-CLMs, Gal20-PTX-CLMs, Gal30-PTX-CLMs, PTX-CLMs and Taxol (PTX dissolved in Cremopher EL and ethanol, v/v = 1:1) were added at a fixed PTX concentration of 5 μg/mL. The cells were then cultured in DMEM medium at 37 °C under 5% CO_2 atmosphere for 4 h. The medium was aspirated and replaced by 100 μL of fresh medium. The cells were cultured for another 44 h (37 °C, 5% CO_2). Then, 10 μL of 3-(4,5-dimethylthiazol-2-yl)-2,5-diphenyltetrazolium bromide (MTT) solution in PBS (5 mg/mL) was added and incubated for 4 h at 37 °C. The medium was aspirated, the MTT-formazan generated by live cells was dissolved in 150 μL of DMSO, and the optical densities at 492 nm of each well were measured using a microplate reader (Multiskan FC, Thermo Scientific). The relative cell viability (%) was determined by comparing the absorbance at 492 nm with control wells containing only cell culture medium. Data are presented as average ± SD (n = 4).

For inhibition experiments, HepG2 cells were pretreated with free LBA (2 mg/mL) for 4 h to block the ASGP-Rs on the cell surface, the media were aspirated and replaced by fresh cell culture media, and then PTX formulations were added.

To determine the effect of the galactose content and crosslinking of micelles on their targetability and on the half inhibitory concentration (IC_{50}) values, antitumor activity of PTX loaded Gal-PTX-CLMs and Gal-PTX-NCLMs with 10%, 20% and 30% Gal contents was evaluated against HepG2 cells at PTX concentrations from 1×10^{-4} to 20 μg/mL.

The cytotoxicity of Gal-CLMs with 10%, 20% and 30% Gal contents to HepG2 and MCF-7 cells was determined in a similar way at micelle concentrations of 0.9, 1.2 and 1.5 mg/mL.

2.7. Pharmacokinetics studies

Pharmacokinetics studies were carried out using Gal20-PTX-CLMs, PTX-CLMs and Taxol in nude mice (dosage: 10 mg PTX equiv./kg, n = 5). At predetermined time points post intravenous administration, *i.e.* 0, 0.167, 0.5, 2, 6, 10 and 24 h for Gal20-PTX-CLM and PTX-CLM groups while 0, 0.0333, 0.0833, 0.1667, 0.5 and 1 h for the Taxol group, blood samples (100 μL) were withdrawn and collected in heparinized tubes. The plasma was isolated by centrifugation at 3000 rpm for 10 min. 25 μL of plasma was homogenized and extracted with 100 μL methanol for 2 min. After centrifugation at 3000 rpm for 10 min, the supernatant was taken and evaporated to dryness under a stream of nitrogen. 100 μL methanol was added to re-dissolve the residue, the solution was filtered through a 0.22 μm filter, and the amount of PTX was determined by HPLC.

2.8. Biodistribution studies

In order to determine the *in vivo* biodistribution of micelles using fluorescence, micelles were labeled with Cy7 employing 5 wt.% Cy7-PEG-PCL. Six mice (tumor size of *ca.* 200 mm^3) were randomly assigned to two groups: (i) Cy7-labeled Gal20-PTX-CLMs, and (ii) Cy7-labeled PTX-CLMs. A single dose of PTX formulation in 0.1 mL of PBS was intravenously administrated *via* the tail vein at a PTX dose of 3 mg/kg body weight. After 5 h, blood samples were collected and mice were sacrificed. The tumor block and organs including the heart, liver, spleen, lung, and kidney were collected, washed and weighted. The samples were homogenized in 4-fold (for plasma) and 2-fold (for tissues) volumes of methanol to extract PTX using a homogenizer (IKA T25) at 18,000 rpm for 15 min followed by centrifugation at 3000 rpm for 20 min. The supernatant was taken and evaporated to dryness under a stream of nitrogen. 100 μL methanol was added to re-dissolve the residue and the amount of PTX was determined by HPLC.

Table 1
Characteristics of Gal-installed PTX-loaded photo-crosslinked micelles.[a]

Entry	Gal content (wt.%)	Size (nm)/PDI[b]		DLC (wt.%)[c]	DLE %[c]
		NCLMs	CLMs		
1	0	104.2/0.13	92.1/0.08	8.36	91.2
2	10	113.5/0.12	101.3/0.11	7.72	83.6
3	20	138.6/0.12	116.7/0.12	6.78	72.7
4	30	157.2/0.08	136.3/0.08	6.17	65.8

[a] Theoretical PTX loading content was 10 wt.%.
[b] Determined by DLS.
[c] Determined by HPLC.

2.9. In vivo antitumor efficacy of PTX-loaded micelles

The *in vivo* antitumor efficacy of PTX-loaded micelles was evaluated using the nude mice bearing the human hepatocellular carcinoma (SMMC-7721) xenograft. The mice were handled under protocols approved by Soochow University Laboratory Animal Center. Nude mice (18–22 g) were injected subcutaneously in the armpit of left posterior limb with 0.2 mL of cell suspension containing 5×10^6 SMMC-7721 cells. Treatments were started after 2 weeks when tumors in the nude mice reached an average volume of 15 mm^3, and this day was designated as day 0. The mice were weighed and randomly divided into five groups of five mice: (i) Gal20-PTX-CLMs, (ii) PTX-loaded CLMs (PTX-CLMs), (iii) Gal decorated PTX-loaded NCLMs (Gal-PTX-NCLMs), (iv) Taxol, and (v) PBS (control). A single dose of PTX formulation in 0.1 mL of PBS (PTX dosage: 3 mg/kg body weight) was intravenously administrated on days 0, 8, 15 and 22. The treatment effect was assessed by measuring the tumor size. Tumor volume was calculated by the formula: $V = 0.5 \times L \times W^2$, wherein L is the tumor dimension at the longest point and W is the tumor measurement at the widest point. On day 32, all mice were sacrificed by cervical vertebra dislocation, and the tumor block was harvested and weighted.

2.10. Histological analysis

On day 32 post treatment, the mice were sacrificed, and the tumor, liver and kidney were excised. The tissues were fixed with 4% paraformaldehyde solution, and embedded in paraffin. The sliced organ tissues (thickness: 4 mm) mounted on the glass slides were stained by hematoxylin and eosin (H&E) and observed using an optical microscope (Olympus BX 41 microscope).

3. Results and discussion

The aim of the present study was to develop integrative degradable micelles for targeted hepatoma chemotherapy. To this end, Gal-installed photo-crosslinked pH-sensitive degradable micelles (Gal-CLMs) were designed and constructed based on the following two amphiphilic block copolymers: (i) PEG-*b*-P(TMBPEC-*co*-AC) (M_n = 5.0–4.2 kg/mol, M_w/M_n = 1.06) that contains acid-labile acetal groups and photo-crosslinkable acryloyl groups on the side chains of the polycarbonate block, and (ii) Gal-PEG-PCL (M_n = 6.0–4.0 kg/mol, M_w/M_n = 1.3) that contains specific targeting ligands to asialoglycoprotein receptor (ASGP-R) over-expressing hepatoma cells. Notably, the PEG chain in Gal-PEG-PCL was devised longer than that in PEG-*b*-P(TMBPEC-*co*-AC) in order to fully expose Gal ligands at the outer surface of micelles for optimal targeting property [10,42].

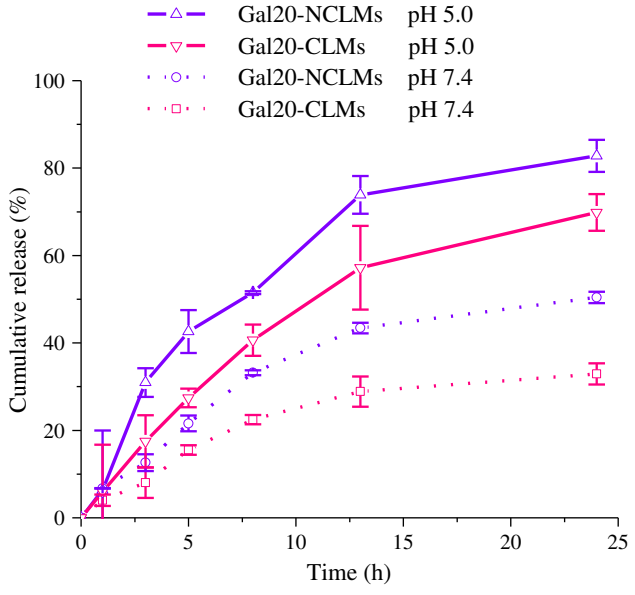

Fig. 1. pH-dependent PTX release from Gal20-PTX-CLMs and Gal20-PTX-NCLMs at a micelle concentration of 32 μg/mL (corresponding to 3.27 μg PTX equiv./mL) and 37 °C.

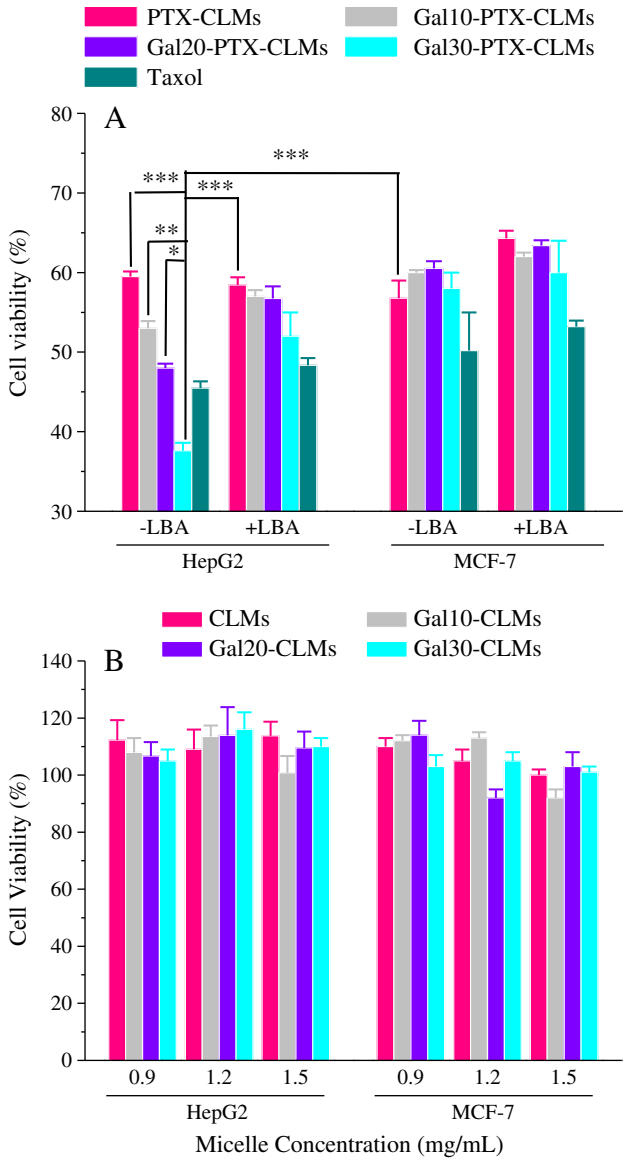

Fig. 2. MTT assays. (A) Antitumor activity of Gal-PTX-CLMs to HepG2 and MCF-7 cells (dosage: 5 μg PTX equiv./mL). The inhibition experiments were performed by pre-treating cells with 2 mg/mL LBA prior to adding micellar drugs. The cells were incubated for 4 h with Gal-PTX-CLMs, media were removed and replenished with fresh culture media, and cells were further cultured for another 44 h. PTX-CLMs and Taxol were used as controls. (B) Cytotoxicity of empty Gal-CLMs to HepG2 and MCF-7 cells following 24 h incubation. Data are presented as mean ± SD (n = 4, Student's test, $^*p < 0.05$, $^{**}p < 0.01$, $^{***}p < 0.001$).

3.1. Micelle preparation, PTX loading and pH-triggered drug release

The co-self-assembly of PEG-*b*-P(TMBPEC-*co*-AC) and Gal-PEG-*b*-PCL copolymers in phosphate buffer (PB, pH 7.4, 10 mM) afforded non-crosslinked micelles (Gal-NCLMs) with low polydispersity indexes (PDIs) of 0.12–0.18 and hydrodynamic sizes of 87.2–134.5 nm, which increased with increasing Gal-PEG-PCL contents from 0 to 30 wt.%. These micelles had low critical micelle concentration (CMC) values of

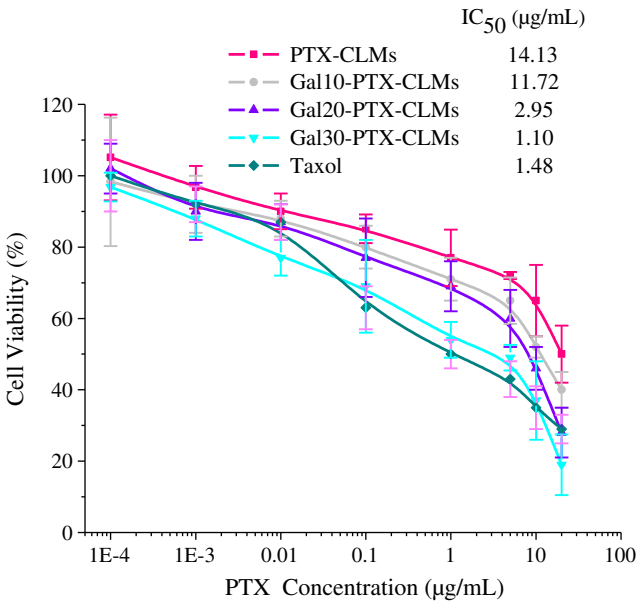

Fig. 3. Cytotoxicity of Gal-PTX-CLMs to HepG2 cells at varying concentrations of 0.0001–20 μg PTX equiv./mL. The cells were incubated with Gal-PTX-CLMs for 4 h, media were removed and replenished with fresh culture media, and cells were further cultured for another 68 h. PTX-CLMs and Taxol were used as controls. The cell viability was determined by MTT assay and data are presented as mean ± SD (n = 4). The inset table lists the IC_{50} values of different formulations.

4.3–6.2 mg/L (Table S1). Notably, micelles were readily crosslinked under UV irradiation (100 mW/cm^2) in the presence of a biocompatible photo-initiator I2959 (0.05 wt.%) in PB (pH 7.4, 10 mM). The micelle sizes were reduced by 5–18 nm after crosslinking (Table S2). TEM micrograph displayed that Gal20-CLMs had a spherical morphology and an average particle size of *ca.* 70 nm (Fig. S1), which was smaller than that determined by DLS likely as a result of dehydration. The crosslinked micelles (Gal-CLMs) showed obviously better colloidal stability than the parent non-crosslinked counterparts, as revealed by experiments against extensive dilution, addition of 4-fold THF, or presence of 10% FBS (Fig. S2).

PTX-loaded Gal-CLMs (Gal-PTX-CLMs) were prepared in a similar way. At a theoretical drug loading content (DLC) of 10 wt.%, decent PTX loading contents of 6.17–8.36 wt.% were achieved (Table 1). Gal-

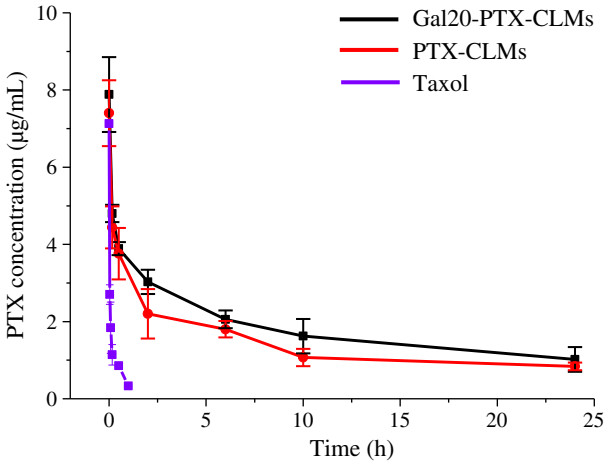

Fig. 4. *In vivo* pharmacokinetics of Gal20-PTX-CLMs, PTX-CLMs and Taxol in mice (means ± SD, n = 5). PTX plasma levels were determined by HPLC. The drug dosage was fixed at 10 mg/kg.

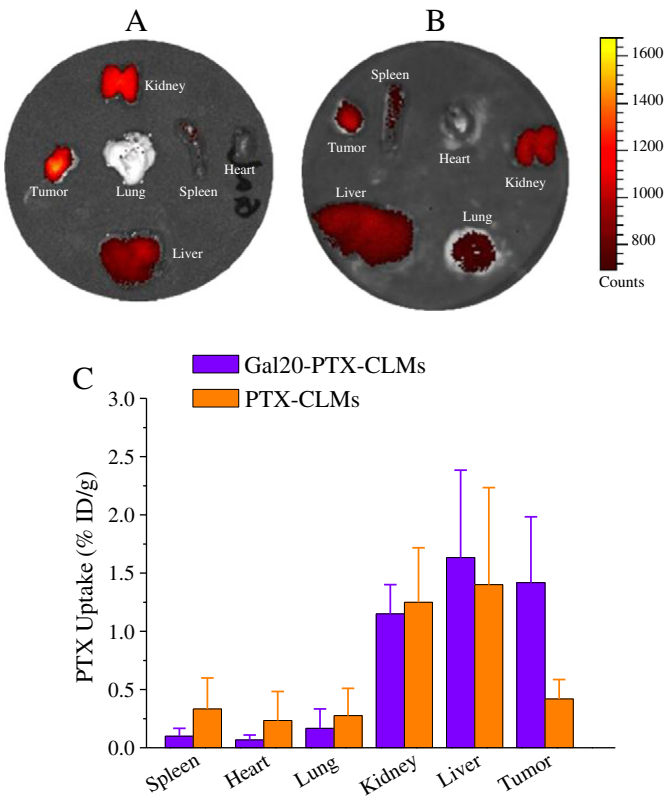

Fig. 5. *In vivo* biodistribution of Cy7-labeled Gal20-PTX-CLMs and PTX-CLMs in SMMC-7721 hepatoma bearing nude mice following 5 h intravenous injection. (A) NIRF image of organs harvested from SMMC-7721 bearing mice treated with Cy7-labeled Gal20-PTX-CLMs; (B) NIRF image of organs harvested from SMMC-7721 bearing mice treated with Cy7-labeled PTX-CLMs; and (C) quantification of PTX accumulated in different organs using HPLC. PTX uptake is expressed as injected dose per gram of tissue (%ID/g). Data are presented as mean ± SD (n = 3).

PTX-CLMs had a narrow distribution (PDI = 0.08–0.12) and slightly larger particle sizes (average diameters: 92.1–136.3 nm) compared to blank Gal-CLMs. The micelle sizes were shrinked by 12–20 nm following UV irradiation. Notably, no PTX leakage occurred during the crosslinking procedure as revealed by HPLC analysis.

The *in vitro* PTX release studies were carried out at a low micelle concentration of 32 μg/mL at pHs 5.0 and 7.4. The results showed that the release of PTX from Gal20-PTX-CLMs at physiological pH was *ca.* 33.9% in 24 h, which was obviously lower than that for Gal20-PTX-NCLMs under otherwise the same conditions (*ca.* 50.4% release in 24 h) (Fig. 1). This inhibited PTX release that was similar to PTX-CLMs (*ca.* 31.2% release in 24 h) as our previous report [24], indicating that incorporation of 20 wt.% Gal-PEG-PCL had little influence on micelle crosslinking. Importantly, drug release from Gal20-PTX-CLMs was significantly enhanced at pH 5.0, in which *ca.* 70% PTX was released in 24 h. This accelerated drug release under mildly acidic conditions was ascribed to the hydrolysis of acetal groups and change of polarity in the micellar core [24]. These results point out that Gal20-PTX-CLMs while being robust with inhibited drug leakage under physiological pH are capable of releasing PTX at endo/lysosomal pH. It should be noted, nevertheless, that Gal20-PTX-NCLMs, though exhibiting an obvious pH-dependent drug release behavior, are not yet ideal in that there is still significant drug leakage at pH 7.4 and drug release at acidic pH remains slow and incomplete.

3.2. Targetability and antitumor activity of Gal-PTX-CLMs toward HepG2 cells

The hepatoma-targeted anti-tumor activity of Gal-PTX-CLMs was studied by MTT assays using HepG2 cells. The cells were first incubated

Table 2
Summary of tumor-to-normal tissue (T/N) distribution ratios of PTX at 5 h after i.v. injection.

	Spleen	Heart	Lung	Kidney	Liver
Gal20-PTX-CLMs	14.17	21.25	8.50	1.23	0.87
PTX-CLMs	1.26	1.80	1.52	0.34	0.30

for 4 h with Gal-PTX-CLMs, PTX-CLMs or Taxol at a PTX dosage of 5 μg/mL, media were aspirated and replenished with fresh culture media, and cells were further cultured for another 44 h. The results showed that Gal-PTX-CLMs with higher Gal contents provoked progressively a higher level of HepG2 cell death (Fig. 2A). For example, with increasing Gal contents from 10% to 20% to 30%, cell viability decreased from *ca.* 53% to 47% to 37%, respectively. Notably, Gal30-PTX-CLMs were significantly more toxic than Taxol. The anti-tumor activity of Gal-PTX-CLMs was reduced by pre-treating HepG2 cells with LBA. In contrast, pre-treatment of HepG2 cells with LBA had little influence on cytotoxicity of PTX-CLMs or Taxol. Moreover, Gal-PTX-CLMs with different Gal contents caused similar cytotoxic effect (*ca.* 60% cell viability) to MCF-7 cells (low ASGP-R expression, negative control), either with or without LBA pre-treatment, under otherwise identical conditions. These results point out that Gal-PTX-CLMs possess apparent targetability to HepG2 cells and can efficiently deliver and release anti-cancer drugs into HepG2 cells inducing effective and specific cell death.

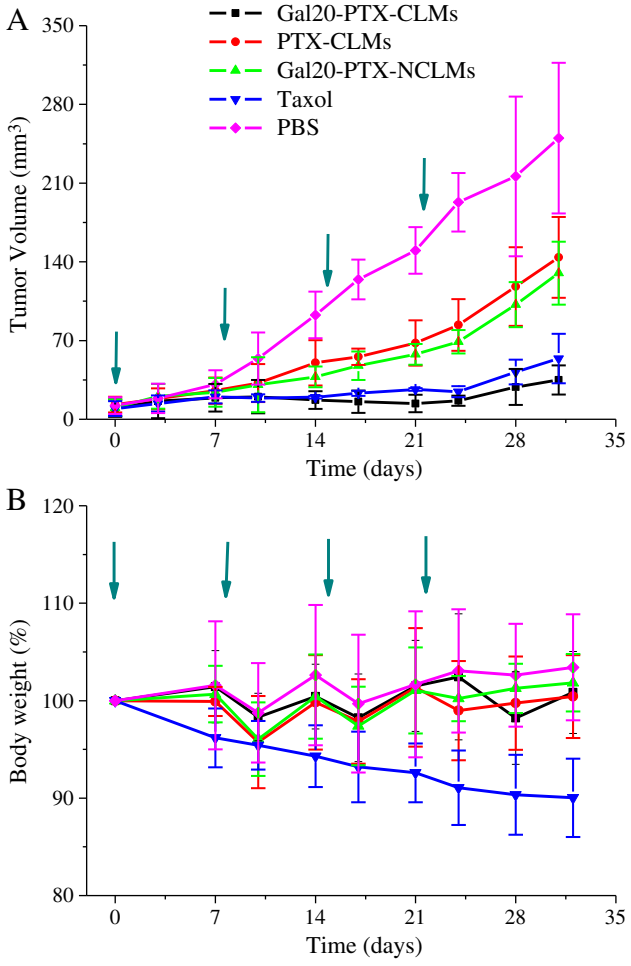

Fig. 6. Tumor volume changes (A) and body weight changes (B) of the SMMC-7721 tumor-bearing nude mice after i.v. injection of the PTX-loaded micelles on days 0, 8, 15 and 22 (dosage: 3 mg PTX equiv./kg body weight, in 0.1 mL PBS).

Similar results were also observed for apoptotic protein-loaded Gal-decorated polymersomes [42]. As expected, Gal-PTX-CLMs were practically nontoxic to both HepG2 and MCF-7 cells (cell viabilities ranging from 95% to 118%) up to a tested concentration of 1.5 mg/mL (Fig. 2B). The half maximal inhibitory concentration (IC_{50}) of Gal-PTX-CLMs to HepG2 cells was determined by MTT assays at PTX concentrations ranging from 0.0001 to 20 μg/mL. The results showed that Gal-PTX-CLMs with Gal contents of 10%, 20% and 30% had decreasing IC_{50} values of 11.70, 2.95 and 1.10 μg PTX equiv./mL, respectively, which were lower than that observed for non-targeting PTX-CLMs (14.10 μg PTX equiv./mL) and approaching that for Taxol (1.48 μg/mL) (Fig. 3). In the following, Gal20-PTX-CLM swere selected for the *in vivo* studies.

3.3. In vivo pharmacokinetics and biodistribution studies

The plasma levels of PTX were determined by HPLC at different time intervals following a single i.v. injection of Gal20-PTX-CLMs, PTX-CLMs and Taxol (10 mg PTX equiv./kg) in nude mice. Notably, Gal20-PTX-CLMs and PTX-CLMs revealed a significantly longer circulation time than Taxol, in which the plasma level of PTX was diminishing following 1 h injection of Taxol, whereas considerable amount of PTX was observed even after 24 h of administering Gal20-PTX-CLMs and PTX-CLMs (Fig. 4). The PTX circulation half-lives for Gal20-PTX-CLMs, PTX-CLMs and Taxol were determined to be 3.86 h, 3.40 h and 0.18 h, respectively.

The *in vivo* biodistribution of Gal20-PTX-CLMs was investigated in human hepatoma SMMC-7721-bearing nude mice. Cy7-labeled Gal20-PTX-CLMs or PTX-CLMs (PTX dosage: 3 mg/kg) were injected intravenously through the tail vein, the mice were sacrificed after 5 h, and the organs were harvested. The *ex vivo* fluorescence images revealed that mice treated with Gal20-PTX-CLMs had strong Cy7 fluorescence in the tumor (Fig. 5A), which was significantly higher than those treated with non-targeting PTX-CLMs (Fig. 5B). It is interesting to note that similar fluorescence was observed for Gal20-PTX-CLMs and PTX-CLMs in the liver, indicating that installation of Gal ligands does not lead to enhanced liver accumulation. It should further be noted that mice treated with Gal20-PTX-CLMs had obviously weaker Cy7 fluorescence in the lung and spleen compared to those with PTX-CLMs. The amounts of PTX accumulated in tumors and major organs such as the spleen, liver,

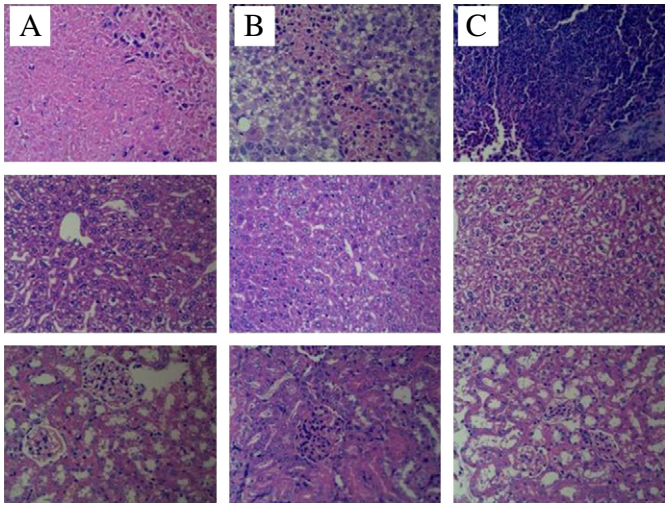

Fig. 7. Images of H&E-stained tumor, liver and kidney sections excised from SMMC-7721 tumor-bearing mice following 32 day treatment with Gal20-PTX-CLMs (A), Taxol (B) and PBS (C). The images from top to bottom were tumor, liver and kidney, respectively. The images were obtained under Olympus BX41 microscope using a 40× objective.

kidney, heart and lung were extracted and quantified using HPLC (Fig. 5C). The results were consistent with the above fluorescence observations. The tumor uptake of PTX was 1.42% of the injected dose per gram of tissue (%ID/g) for Gal20-PTX-CLMs, which was over 3 times higher than that for PTX-CLMs (0.41%ID/g). While similar in the kidney and liver, lower PTX levels were observed for Gal20-PTX-CLMs in the spleen, heart and lung than for PTX-CLMs. The tumor-to-normal tissue (T/N) distribution ratios of PTX are summarized in Table 2. These collected data demonstrated that Gal20-PTX-CLMs could in general reduce PTX uptake by healthy organs or tissues particularly the spleen, heart, and lung while largely increase PTX accumulation in the solid tumors.

3.4. In vivo therapeutic efficacy of Gal-PTX-CLMs

The hepatoma-targeting antitumor activity of Gal20-PTX-CLMs was evaluated using SMMC-7721 bearing nude mice. The mice were dosed on days 0, 8, 15 and 22 with 3 mg PTX equiv./kg. Tumor volume was monitored over a period of 32 days. The results showed fast tumor growth for mice receiving only PBS, with tumor volume reaching approximately 250 mm^3 on day 32 (Fig. 6A). Remarkably, mice treated with Gal-PTX-CLMs showed almost complete inhibition of tumor growth in the first 24 days. In contrast, continuous tumor growth was observed for mice treated with PTX-CLMs (non-targeting control) and Gal20-PTX-NCLMs (non-crosslinked controls). Moreover, Gal-PTX-CLMs caused also slightly better tumor inhibition than Taxol. The mice treated with Gal20-PTX-CLMs, PTX-CLMs, Gal20-PTX-NCLMs, and Taxol had an average tumor volume of *ca.* 35 mm^3, 144 mm^3, 130 mm^3, and 45 mm^3, respectively, on day 32 (Fig. 6A). In close correlation with tumor volumes, average tumor block weights of mice treated with Gal20-PTX-CLMs, PTX-CLMs, Gal20-PTX-NCLMs, Taxol and PBS were shown to be 0.054, 0.132, 0.122, 0.062 and 0.253 g, respectively. The inferior antitumor efficacy of PTX-CLMs to Gal20-PTX-CLMs was most likely due to the poor cellular uptake by SMMC-7721 cells, signifying the importance of introducing targeting ligands to micellar drugs. The enhanced antitumor efficacy of Gal20-PTX-CLMscompared with Gal20-PTX-NCLMs highlights the significant role of micelle stabilization. It should further be noted that SMMC-7721 bearing nude mice treated with all micellar formulations exhibited little body weight change in 32 days, whereas *ca.* 10% body weight loss was observed for mice treated with Taxol (Fig. 6B), indicating that these micellar formulations have lower side effects and better drug tolerance compared to Taxol.

To further investigate the therapeutic performance of active targeting systems, we have also carried out histological analysis using H&E staining. The results showed that tumor tissues of Gal20-PTX-CLM treated mice underwent significantly more extensive apoptosis than those with Taxol (Fig. 7). Moreover, it is remarkable to note that Gal20-PTX-CLMs caused much less damage to the liver and kidney compared to Taxol. Fig. 5 shows that Gal20-PTX-CLMs had a similar accumulation level to tumors in the liver and kidney. The less liver and kidney damage observed for Gal20-PTX-CLMs is most likely because normal liver and kidney cells cannot efficiently take up Gal20-PTX-CLMs and the drug cannot readily be released under physiological conditions as a result of core-crosslinking. These results demonstrate that active targeting core-crosslinked pH-responsive degradable micelles can not only enhance therapeutic efficacy of anticancer drugs but also largely decrease their side effects.

4. Conclusions

We have demonstrated that galactose-installed core-crosslinked pH-sensitive degradable micelles mediate active targeting chemotherapy of hepatocellular carcinoma in mice, resulting in potent inhibition of tumor growth and alleviation of systemic side effects. This is a first development of integrative degradable micellar systems for effective hepatoma-targeting chemotherapy. These multifunctional micellar systems have integrated following unique features: (i) they have excellent stability with inhibited drug leakage under physiological conditions or in circulation owing to chemical crosslinking of the micellar core; (ii) they can be specifically and efficiently taken up by target hepatoma cells *via* the receptor-mediated mechanism; (iii) drug release is boosted in the endo/lysosomal compartments by acid-triggered hydrolysis of acetals in the micellar core, leading to potent antitumor activity; and (iv) they are degradable, non-toxic and easy to prepare. Remarkably, our results have shown that these integrative degradable micellar systems cause little damage to the kidney and liver, most likely due to poor uptake by normal kidney and liver cells. Hence, ligand-installed photo-crosslinked pH-responsive degradable micelles provide an interesting platform for targeted cancer chemotherapy.

Acknowledgments

This work is financially supported by research grants from the National Natural Science Foundation of China (NSFC 51173126, 51273139, 51103093, 51273137, 51003070 and 81261120557), the National Science Fund for Distinguished Young Scholars (NSFC 51225302), Jiangsu Specially-Appointed Professor Program, Ph.D. Programs Foundation of Ministry of Education of the People's Republic of China (20133201110005), and a project funded by the Priority Academic Program Development (PAPD) of Jiangsu Higher Education Institutions.

Appendix A. Supplementary data

Supplementary data to this article can be found online at http://dx.doi.org/10.1016/j.jconrel.2014.05.016.

References

[1] D. Peer, J.M. Karp, S. Hong, O.C. FaroKhzad, R. Margalit, R. Langer, Nanocarriers as an emerging platform for cancer therapy, Nat. Nanotechnol. 2 (2007) 751–760.
[2] J. Gong, M. Chen, Y. Zheng, S. Wang, Y. Wang, Polymeric micelles drug delivery system in oncology, J. Control. Release 159 (2012) 312–323.
[3] G. Gaucher, R.H. Marchessault, J.-C. Leroux, Polyester-based micelles and nanoparticles for the parenteral delivery of taxanes, J. Control. Release 143 (2010) 2–12.
[4] J. Nicolas, S. Mura, D. Brambilla, N. Mackiewicz, P. Couvreur, Design, functionalization strategies and biomedical applications of targeted biodegradable/biocompatible polymer-based nanocarriers for drug delivery, Chem. Soc. Rev. 42 (2013) 1147–1235.
[5] C. Deng, Y.J. Jiang, R. Cheng, F.H. Meng, Z.Y. Zhong, Biodegradable polymeric micelles for targeted and controlled anticancer drug delivery: promises, progress and prospects, Nano Today 7 (2012) 467–480.
[6] S.C. Owen, D.P.Y. Chan, M.S. Shoichet, Polymeric micelle stability, Nano Today 7 (2012) 53–65.
[7] R.K. O'Reilly, C.J. Hawker, K.L. Wooley, Cross-linked block copolymer micelles: functional nanostructures of great potential and versatility, Chem. Soc. Rev. 35 (2006) 1068–1083.
[8] E.S. Read, S.P. Armes, Recent advances in shell cross-linked micelles, Chem. Commun. (2007) 3021–3035.
[9] C.F. van Nostrum, Covalently cross-linked amphiphilic block copolymer micelles, Soft Matter 7 (2011) 3246–3259.
[10] R. Yang, F. Meng, S. Ma, F. Huang, H. Liu, Z. Zhong, Galactose-decorated cross-linked biodegradable poly(ethylene glycol)-b-poly(epsilon-caprolactone) block copolymer micelles for enhanced hepatoma-targeting delivery of paclitaxel, Biomacromolecules 12 (2011) 3047–3055.
[11] J. Xiong, F. Meng, C. Wang, R. Cheng, Z. Liu, Z. Zhong, Folate-conjugated crosslinked biodegradable micelles for receptor-mediated delivery of paclitaxel, J. Mater. Chem. 21 (2011) 5786–5794.
[12] D. Kim, E.S. Lee, K.T. Oh, Z.G. Gao, Y.H. Bae, Doxorubicin-loaded polymeric micelle overcomes multidrug resistance of cancer by double-targeting folate receptor and early endosomal pH, Small 4 (2008) 2043–2050.
[13] F. Wang, Y.-C. Wang, S. Dou, M.-H. Xiong, T.-M. Sun, J. Wang, Doxorubicin-tethered responsive gold nanoparticles facilitate intracellular drug delivery for overcoming multidrug resistance in cancer cells, ACS Nano 5 (2011) 3679–3692.
[14] M. Kamimura, T. Furukawa, S.-I. Akiyama, Y. Nagasaki, Enhanced intracellular drug delivery of pH-sensitive doxorubicin/poly(ethylene glycol)-block-poly(4-vinylbenzylphosphonate) nanoparticles in multi-drug resistant human epidermoid KB carcinoma cells, Biomater. Sci. 1 (2013) 361–367.
[15] L.L. Wu, Y. Zou, C. Deng, R. Cheng, F.H. Meng, Z.Y. Zhong, Intracellular release of doxorubicin from core-crosslinked polypeptide micelles triggered by both pH and reduction conditions, Biomaterials 34 (2013) 5262–5272.

[16] R.R. Wei, L. Cheng, M. Zheng, R. Cheng, F.H. Meng, C. Deng, Z.Y. Zhong, Reduction-responsive disassemblable core-cross-linked micelles based on poly(ethylene glycol)-b-poly(N-2-hydroxypropyl methacrylamide)–lipoic acid conjugates for triggered intracellular anticancer drug release, Biomacromolecules 13 (2012) 2429–2438.
[17] Y.-L. Li, L. Zhu, Z.Z. Liu, R. Cheng, F.H. Meng, J.-H. Cui, S.-J. Ji, Z.Y. Zhong, Reversibly stabilized multifunctional dextran nanoparticles efficiently deliver doxorubicin into the nuclei of cancer cells, Angew. Chem. Int. Ed. 48 (2009) 9914–9918.
[18] Y. Li, K. Xiao, J. Luo, W. Xiao, J.S. Lee, A.M. Gonik, J. Kato, T.A. Dong, K.S. Lam, Well-defined, reversible disulfide cross-linked micelles for on-demand paclitaxel delivery, Biomaterials 32 (2011) 6633–6645.
[19] A.N. Koo, K.H. Min, H.J. Lee, S.-U. Lee, K. Kim, I.C. Kwon, S.H. Cho, S.Y. Jeong, S.C. Lee, Tumor accumulation and antitumor efficacy of docetaxel-loaded core-shell-corona micelles with shell-specific redox-responsive cross-links, Biomaterials 33 (2012) 1489–1499.
[20] S. Cajot, N. Lautram, C. Passirani, C. Jerome, Design of reversibly core cross-linked micelles sensitive to reductive environment, J. Control. Release 152 (2011) 30–36.
[21] S.J. Lee, K.H. Min, H.J. Lee, A.N. Koo, H.P. Rim, B.J. Jeon, S.Y. Jeong, J.S. Heo, S.C. Lee, Ketal cross-linked poly(ethylene glycol)–poly(amino acid)s copolymer micelles for efficient intracellular delivery of doxorubicin, Biomacromolecules 12 (2011) 1224–1233.
[22] Y. Li, W. Xiao, K. Xiao, L. Berti, J. Luo, H.P. Tseng, G. Fung, K.S. Lam, Well-defined, reversible boronate crosslinked nanocarriers for targeted drug delivery in response to acidic pH values and cis-diols, Angew. Chem. Int. Ed. 51 (2012) 2864–2869.
[23] M. Talelli, M. Iman, A.K. Varkouhi, C.J.F. Rijcken, R.M. Schiffelers, T. Etrych, K. Ulbrich, C.F. van Nostrum, T. Lammers, G. Storm, W.E. Hennink, Core-crosslinked polymeric micelles with controlled release of covalently entrapped doxorubicin, Biomaterials 31 (2010) 7797–7804.
[24] Y.L. Wu, W. Chen, F.H. Meng, Z.J. Wang, R. Cheng, C. Deng, H.Y. Liu, Z.Y. Zhong, Core-crosslinked pH-sensitive degradable micelles: a promising approach to resolve the extracellular stability versus intracellular drug release dilemma, J. Control. Release 164 (2012) 338–345.
[25] Y.D. Gu, Y.N. Zhong, F.H. Meng, R. Cheng, C. Deng, Z.Y. Zhong, Acetal-linked paclitaxel prodrug micellar nanoparticles as a versatile and potent platform for cancer therapy, Biomacromolecules 14 (2013) 2772–2780.
[26] H. Kenmotsu, M. Yasunaga, K. Goto, T. Nagano, J.-I. Kuroda, Y. Koga, A. Takahashi, Y. Nishiwaki, Y. Matsumura, The antitumor activity of NK012, an SN-38-incorporating micelle, in combination with bevacizumab against lung cancer xenografts, Cancer 116 (2010) 4597–4604.
[27] J.S. Lee, T. Groothuis, C. Cusan, D. Mink, J. Feijen, Lysosomally cleavable peptide-containing polymersomes modified with anti-EGFR antibody for systemic cancer chemotherapy, Biomaterials 32 (2011) 9144–9153.
[28] N. Nasongkla, X. Shuai, H. Ai, B.D. Weinberg, J. Pink, D.A. Boothman, J.M. Gao, cRGD-functionalized polymer micelles for targeted doxorubicin delivery, Angew. Chem. Int. Ed. 43 (2004) 6323–6327.
[29] Q. Xu, Y. Liu, S. Su, W. Li, C. Chen, Y. Wu, Anti-tumor activity of paclitaxel through dual-targeting carrier of cyclic RGD and transferrin conjugated hyperbranched copolymer nanoparticles, Biomaterials 33 (2012) 1627–1639.
[30] C.K. Huang, C.L. Lo, H.H. Chen, G.H. Hsiue, Multifunctional micelles for cancer cell targeting, distribution imaging, and anticancer drug delivery, Adv. Funct. Mater. 17 (2007) 2291–2297.
[31] D.Q. Wu, B. Lu, C. Chang, C.S. Chen, T. Wang, Y.Y. Zhang, S.X. Cheng, X.J. Jiang, X.Z. Zhang, R.X. Zhuo, Galactosylated fluorescent labeled micelles as a liver targeting drug carrier, Biomaterials 30 (2009) 1363–1371.
[32] Z. Xiao, O.C. Farokhzad, Aptamer-functionalized nanoparticles for medical applications: challenges and opportunities, ACS Nano 6 (2012) 3670–3676.
[33] O.C. Farokhzad, J.J. Cheng, B.A. Teply, I. Sherifi, S. Jon, P.W. Kantoff, J.P. Richie, R. Langer, Targeted nanoparticle-aptamer bioconjugates for cancer chemotherapy *in vivo*, Proc. Natl. Acad. Sci. U. S. A. 103 (2006) 6315–6320.
[34] J. Yue, S. Liu, R. Wang, X. Hu, Z. Xie, Y. Huang, X. Jing, Transferrin-conjugated micelles: enhanced accumulation and antitumor effect for transferrin-receptor-overexpressing cancer models, Mol. Pharm. 9 (2012) 1919–1931.
[35] Y. Li, Z.-Y. Tang, J.-X. Hou, Hepatocellular carcinoma: insight from animal models, Nat. Rev. Gastroenterol. Hepatol. 9 (2012) 32–43.
[36] P.A. Ma, S. Liu, Y.B. Huang, X.S. Chen, L.P. Zhang, X.B. Jing, Lactose mediated liver-targeting effect observed by ex vivo imaging technology, Biomaterials 31 (2010) 2646–2654.
[37] A. David, P. Kopeckova, A. Rubinstein, J. Kopecek, Enhanced-biorecognition and internalization of HPMA copolymers containing multiple or multivalent carbohydrate side-chains by human hepatocarcinoma cells, Bioconjug. Chem. 12 (2001) 890–899.
[38] J. Ding, C. Xiao, Y. Li, Y. Cheng, N. Wang, C. He, X. Zhuang, X. Zhu, X. Chen, Efficacious hepatoma-targeted nanomedicine self-assembled from galactopeptide and doxorubicin driven by two-stage physical interactions, J. Control. Release 169 (2013) 193–203.
[39] P.J. Julyan, L.W. Seymour, D.R. Ferry, S. Daryani, C.M. Boivin, J. Doran, M. David, D. Anderson, C. Christodoulou, A.M. Young, S. Hesslewood, D.J. Kerr, Preliminary clinical study of the distribution of HPMA copolymers bearing doxorubicin and galactosamine, J. Control. Release 57 (1999) 281–290.
[40] F. Suriano, R. Pratt, J.P.K. Tan, N. Wiradharma, A. Nelson, Y.-Y. Yang, P. Dubois, J.L. Hedrick, Synthesis of a family of amphiphilic glycopolymers via controlled ring-opening polymerization of functionalized cyclic carbonates and their application in drug delivery, Biomaterials 31 (2010) 2637–2645.
[41] L.W. Seymour, D.R. Ferry, D. Anderson, S. Hesslewood, P.J. Julyan, R. Poyner, J. Doran, A.M. Young, S. Burtles, D.J. Kerr, Hepatic drug targeting: phase I evaluation of polymer-bound doxorubicin, J. Clin. Oncol. 20 (2002) 1668–1676.
[42] X.Y. Wang, H.L. Sun, F.H. Meng, R. Cheng, C. Deng, Z.Y. Zhong, Galactose-decorated reduction-sensitive degradable chimaeric polymersomes as a multifunctional nanocarrier to efficiently chaperone apoptotic proteins into hepatoma cells, Biomacromolecules 14 (2013) 2873–2882.
[43] Y.N. Zhong, C. Wang, L. Cheng, F.H. Meng, Z.Y. Zhong, Z. Liu, Gold nanorod-cored biodegradable micelles as a robust and remotely controllable doxorubicin release system for potent inhibition of drug-sensitive and -resistant cancer cells, Biomacromolecules 14 (2013) 2411–2419.
[44] W. Chen, Y. Zou, J.N. Jia, F.H. Meng, R. Cheng, C. Deng, J. Feijen, Z.Y. Zhong, Functional poly(epsilon-caprolactone)s via copolymerization of epsilon-caprolactone and pyridyl disulfide-containing cyclic carbonate: controlled synthesis and facile access to reduction-sensitive biodegradable graft copolymer micelles, Macromolecules 46 (2013) 699–707.
[45] W. Chen, P. Zhong, F.H. Meng, R. Cheng, C. Deng, F. Jan, Z.Y. Zhong, Redox and pH-responsive degradable micelles for dually activated intracellular anticancer drug release, J. Control. Release 169 (2013) 171–179.
[46] H.L. Sun, B.N. Guo, R. Cheng, F.H. Meng, H.Y. Liu, Z.Y. Zhong, Biodegradable micelles with sheddable poly(ethylene glycol) shells for triggered intracellular release of doxorubicin, Biomaterials 30 (2009) 6358–6366.